Synthesis of Dendrimer-Type Poly(ethylene glycol) Structures from Plasma-Functionalized Silicone Rubber Surfaces

H. Jiang,[1] S. Manolache,[1] A. C. Wong,[2] F. S. Denes[1,3]

[1]*Center for Plasma-Aided Manufacturing, University of Wisconsin-Madison, Madison, Wisconsin*
[2]*Food Research Institute, University of Wisconsin-Madison, Madison, Wisconsin*
[3]*Department of Biological Systems Engineering, University of Wisconsin-Madison, Madison, Wisconsin*

Received 23 August 2005; revised 2 February 2006; accepted 5 February 2006
DOI 10.1002/app.24472
Published online in Wiley InterScience (www.interscience.wiley.com).

ABSTRACT: PEG oligomers were covalently attached to nonequilibrium, low-pressure, RF-plasma-functionalized silicone medical- and industrial-grade silicon rubber surfaces, in the absence and presence of linear and branched polyglycidol spacer-chain molecules. All surface-modification reactions were carried out in a two-step process involving an initial argon–plasma activation of the surface, followed by ''*in situ*'' reaction with dichlorosilane in the absence of the discharge, and the attachment of PEG molecules or the graft polymerization of polyglycidol structures, and the attachment of PEG molecules. The surface of substrates was analyzed after each reaction step, using ESCA, ATR-FTIR, and AFM. It was found that PEG molecules directly attached to medical-grade silicone rubber surface as brush-type structures, and generate stronger antifouling characteristics in comparison to similar structures generated on food-grade substrates. The presence of additives on the food-grade silicon rubber surfaces that might be etched and removed during the postplasma washing cycles could contribute to a less efficient attachment of PEG molecules. Surfaces resulting from PEG molecules attached through intermediate, linear, and branched polyglycidol molecules did not reduce bacterial attachment. It is suggested that macromolecular entanglement might be responsible for this behavior. © 2006 Wiley Periodicals, Inc. J Appl Polym Sci 102: 2324–2337, 2006

Key words: dendrimers; polyethers; ring-opening polymerization; plasma functionalization; antifouling thin layers

INTRODUCTION

The mechanism of microorganism adhesion is a very complex phenomenon and is not yet fully understood. Adhesion can be affected by many factors, including Brownian motion, van der Waals and electrostatic forces, gravitation, diffusion, convection or intrinsic motility, fluid forces, pH, temperature, presence of various nutrients and adhesion proteins, and cell surface structure. Short range forces, such as dipole–dipole interactions, hydrogen, ionic and covalent bonding, and hydrophobic interactions are also involved in the adhesion mechanisms.[1–6]

Poly(ethylene glycol) (PEG) is a synthetic, nontoxic, water-soluble polymer.[7] PEG, when attached to various material surfaces, has demonstrated an antifouling capability. It is suggested that heavy hydration, densely packed structure, neutrality, conformational flexibility, and high chain mobility should be the required characteristics of surface-bound PEG molecules for effective inhibition of protein and microorganism adsorption.[8,9] The absence of binding sites might also play a significant role in the microorganism-repelling process.

Several approaches have been developed to produce PEG-coated surfaces, including physical adsorption[10,11] and covalent grafting reaction mechanism.[6,12] Functionalities present as end groups of the PEG chains are usually involved in the synthesis of PEG conjugates, block copolymers, and covalent attachment of PEG molecules to various surfaces.[13]

Based on conformational freedom considerations, it was hypothesized that branched PEG structures have smaller exclusion volumes and, as a consequence, these structures should be less effective in protein rejection than their linear counterparts of similar molecular weight. It is suggested that the presence of high surface density of mobile PEG chains is required on substrate surfaces, for the development of an effective protein rejection behavior. Most conventional procedures considered for PEG attachment suffer from low reproducibility and poor spatially controlled deposition.[6,12,14–19] In addition, covalent grafting of PEG or its modified versions, such as copolymer structures, can only be achieved using functional polymer–substrate surfaces.[6,12]

Brush-type PEG surface layers could play an important role in the design and development of antifouling

Correspondence to: F. S. Denes (denes@engr.wisc.edu).

surfaces. Covalently linked polyglycidol (PG) brushes were prepared, for instance, at 110°C, on Si/SiO_2 surfaces, using anionic ring-opening polymerization. These dendritic and hyperbranched polymer structures led to higher reactive group (e.g., —OH groups) densities on the substrate surface, in comparison to their linear counterparts, and could open up new avenues for surface chemistry and for the synthesis of thin layers. Applications include controlled drug delivery by taking advantage of the encapsulation of active biomolecules into the dendritic layers.[20]

To circumvent the negative influence of a smaller size-exclusion volume of dendritic and hyperbranched structures, and keeping at the same time high reactive-group densities, in this study, PEG molecules also were covalently attached as end chains to the branched polymeric network. It was assumed that a sufficiently thick PEG surface layer could decrease the interaction of proteins and cells with the substrate.

Surface functionalization of inert polymeric materials, including polyethylene, polypropylene, silicone rubber (SR), and poly(tetrafluoro ethylene), cannot be accomplished easily using conventional wet chemical approaches. Cold-plasma technique was selected for the surface functionalization of SR substrates, because it allows the surface modification of even the most inert substrates. The active species of the discharge have energy levels that are comparable with common bond energies of organic structures containing main group elements. The plasma functionalization approach is also a heterogeneous, dry reaction mechanism, which involves minimal amounts of reactants.

PEG covalent grafting on SR has not been reported. In this contribution, plasma-enhanced synthesis of covalently linked PEG and dendrimer-type PEG layers onto SR surfaces is described.

EXPERIMENTAL

Materials

Poly(ethylene glycol) (PEG), MW 400 and 600, dichlorosilane (DS), trifluoroacetic anhydride (TFAA), glycidol (2-epoxy-1-propanol), methanol, and sodium hydroxide were purchased from Aldrich Chemical (Milwaukee, WI). Fluorescamine was purchased from Molecular Probes (Eugene, OR). Argon and oxygen used as the gas media for plasma-enhanced reactor-cleaning operations were obtained from AGA-Linde (Wilmington, DE). Medical- and food-grade silicone rubber (MSR, FSR) were obtained from McMaster-Carr Supply Company (Chicago, IL). All SR substrates were cut into 1×1 cm^2 samples. The SR chips were washed in a hot alkaline detergent (Micro; International Products, Trenton, NJ) for 30 min, rinsed five times in distilled water, and air-dried before use.

Synthesis pathways

Surface implantation of Si—Cl groups onto SR substrates was carried out in a capacitively coupled (9-cm disc-shaped lower electrode and 12.5-cm upper disc-shaped electrodes separated by a 3-cm gap), 40 kHz, cylindrical, glass plasma reactor (Fig. 1). The reactor is composed of a Pyrex-glass cylindrical chamber that is equipped with two disc-shaped stainless steel electrodes. The upper, grounded electrode is connected to the gas-feeding installation, vacuum system, and pressure gauge. The lower electrode serves as the substrate holder and is connected to the RF-power supply.

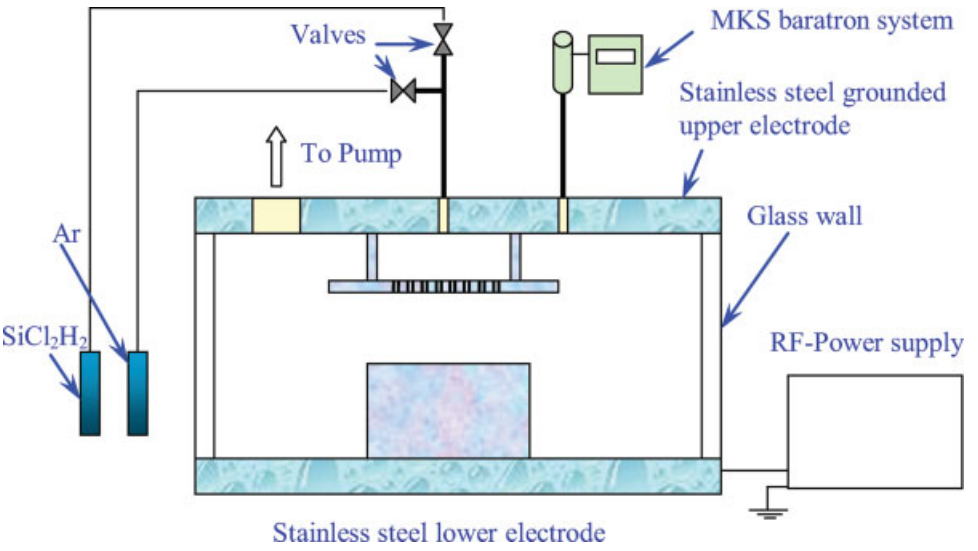

Figure 1 Schematic diagram of capacitively coupled RF-plasma reactor. [Color figure can be viewed in the online issue, which is available at www.interscience.wiley.com.]

In a typical experiment, the reactor with a specific substrate positioned on the lower, stressed electrode was evacuated to base pressure, and the selected argon working pressure was created. The plasma was then initiated and sustained for the required treatment period. Consecutive to the plasma, DS was introduced into the chamber under vacuum (>1000 mTorr) for at least 1 min. In the next step, the reactor was evacuated to base pressure and re-pressurized to atmospheric pressure using argon. The argon–plasma-exposed and DS-treated substrates were coated with degassed PEG under argon protection, without removing them from the reaction chamber. All samples were removed from the reactor and kept in a vacuum oven overnight at 45°C.

The following plasma parameters were employed: base pressure in the absence of plasma: 20 mTorr; argon pressure in the absence of plasma 100 mTorr, argon pressure in the presence of plasma: 110 mTorr; RF power dissipated to the electrodes, 50 W; reaction time, 1 min.

The substrates were removed from PEG solution, washed with distilled water, dried, and subjected to analytical evaluation and assessment of antifouling activity.

The —Si—OH-bearing SR chips were treated in the next step with 20 mL of sodium methoxide (0.043 mol NaOH + 1 L 99.8% anhydrous methanol) solution for 1 h at 60–70 °C under N_2 atmosphere. The chips were then removed from the solution and washed with anhydrous methanol two times, and dried under vacuum at 100°C for 15 min. The functionalized SR chips were immersed into freshly distilled glycidol and kept at 110°C for 15 min. The chips were washed with water/ethanol and dried under vacuum.

Glycidol-grafted chips were immersed into the epichlorohydrin (ECH) at 60–70°C for 1 h under the protection of N_2, then washed with acetone three times, and dried in a vacuum oven at 60–70°C for 15 min. The oxirane-group terminated structures were reacted with PEG according to the following procedure: oxirane-terminated chips were placed into PEG (MW, 400) at 60–70°C overnight under vacuum. The chips were washed with distilled water six times, and dried in a vacuum oven at 60–70°C for 15 min.

Surface analyses

The relative surface atomic concentrations and the relative ratios of carbon, oxygen, silicon, and fluorine atoms present in nonequivalent atomic environments, of unmodified and plasma-modified surfaces, were analyzed by survey and high resolution (HR) electron spectroscopy for chemical analysis (ESCA), using a Perkin–Elmer Physical Electronics 5400 Small Area Spectrometer (Mg source; 15 kV; 300 W; pass energy, 89.45 eV; angle, 45°; Perkin–Elmer (Palo Alto, CA)). Carbon (C_{1s}), oxygen (O_{1s}), silicon (Si_{2p}), and fluorine (F_{1s}) atomic compositions were evaluated, and the peaks corresponding to atoms located in nonequivalent positions were analyzed. To correct for surface-charge-origin binding energy (BE) shifts, calibrations were performed based on the well-known C—Si (C_{1s}) and Si—C (Si_{2p}) peaks.

All ATR-FTIR experiments were conducted using ATI-Mattson Research Series IR instrument, provided with a GRASEBY-Special Benchmark Series ATR in-compartment P/N/11160 unit (Mattson Instruments, Madison, WI) under a nitrogen blanket, generated from a flow-controlled liquid nitrogen tank. Differential ATR-FTIR spectra were obtained by subtraction of the reference spectra of unmodified substrates from the spectra of modified samples, to eliminate the substrate signals. Data were collected in the 600–4000 cm^{-1} wavenumber region, with 250 scans for each sample.

Morphologies of plasma-exposed polymer surfaces and those of the PEG-like structures were analyzed using atomic force microscopy (AFM), employing a Digital Instrument Nanoscope IV microscope (scan rate, 1.9 Hz; sampling number, 512; Santa Barbara, CA).

Chemical derivatization using TFAA coupled with ESCA analysis was performed on hydroxyl groups that were plasma-attached onto silicon–rubber surfaces. All derivatization reactions were performed using a vapor phase process in a vacuum desiccator, equipped with a vacuum line and with a TFAA cylinder.

Primary aliphatic amine functionalities were labeled using fluorescamine. The fluorescamine/acetone solution was sprayed over the samples three times, using a Gelman Chromist aerosol propellant attached to a polypropylene bottle. The fluorescence was revealed with the aid of a UBL 21 Black-Ray UV-Lamp (UVP, San Gabriel, CA) and a FCR-10 photo camera (Fotodyne, Hartland, WI).

Evaluation of antifouling activity

Five strains of *Listeria monocytogenes*, Scott A (serotype 4b, human isolate), JBL 1157 (serotype 4b, processed meat), CLIP 23485 (unknown serotype, liver pâté), F6900 (serotype 1/2a, human), and F8964 (serotype 1/2b, human), which are human and food isolates from listeriosis outbreaks, were grown overnight in trypticase soy broth (Becton Dickinson Microbiology Systems, Cockeysville, MD) at 37°C. The strains were combined to form a five-strain cocktail.

The ability to inhibit biofilm formation by *L. monocytogenes* on MSR and FSR substrates coated with PEG film was evaluated. A 100 μL portion of the combined culture was transferred to a sterile flask containing 50 mL extracellular polysaccharide media with yeast extract.[21] SR chips were glued on to autoclaved cover slides and were put inside the flasks,

then incubated at 27°C at 100 rpm in a gyrotory water bath shaker (model G76, New Brunswick Scientific, Edison, NJ) for 48 h. The chips were removed from the flasks and rinsed in 25 mL of 10 m*M* sodium phosphate-buffered saline (PBS, pH 7.2) by manually shaking the petri dish three times clockwise and three times counterclockwise. The surface of each chip was first swapped five times in a straight direction from left to right. Then the swab and the chip were rotated to 90°, and the surface of the chip was swabbed for another five times in the same way. Each chip surface was swabbed 20 times with one swab (five times from each of the four directions). Altogether, two swabs were used to remove bacteria from each chip. Swab tips were broken off into a tube containing 5 mL PBS and glass beads, and vortexed for 30 s to detach the bacteria. The number of organisms was evaluated by plating appropriate dilutions onto duplicate brain heart infusion agar plates. The plates were incubated at 30°C for 48 h, and the numbers of colony forming units (CFUs) developed were counted.

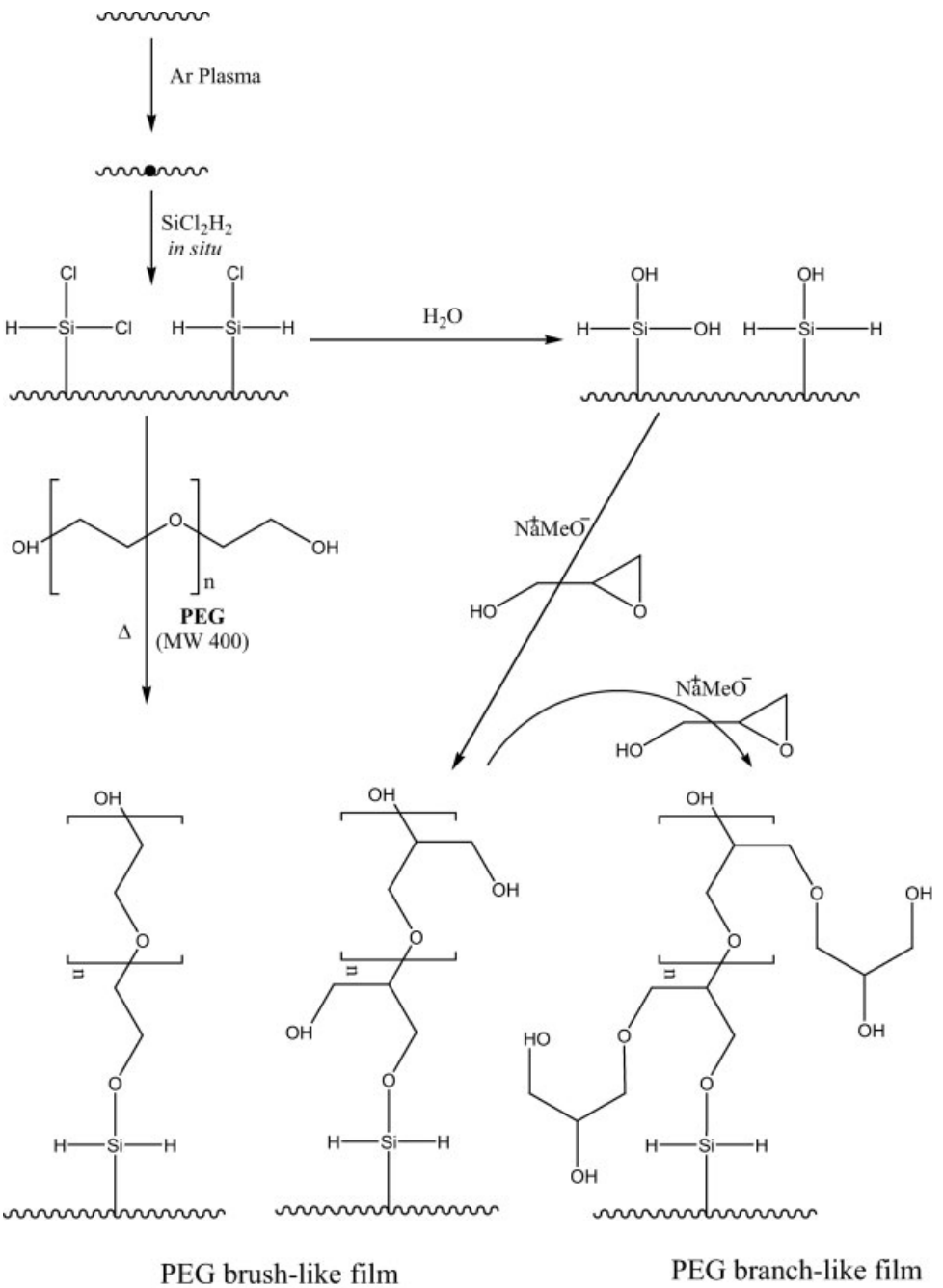

Figure 2 Reaction mechanism of plasma-enhanced surface functionalization.

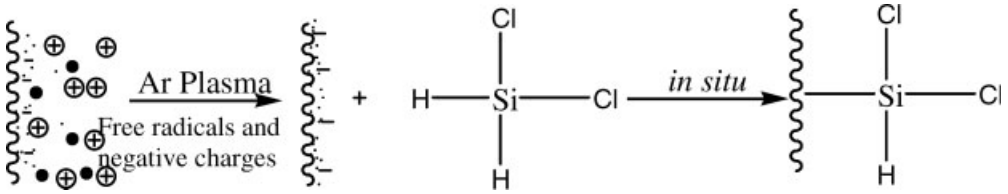

Scheme 1

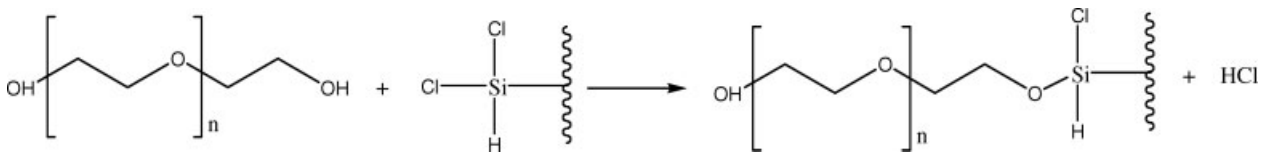

Scheme 2

RESULTS AND DISCUSSION

Synthesis of PEG-like layers, include a four-step process: (1) argon–plasma enhanced surface functionalization of SR sample surfaces, which is followed by *in situ* reaction with DS that results in the implantation of Si—OH surface functionalities, *ex-situ* generation, in the absence of plasma, of (2) PG- and (3) ECH-based intermediate brush structures, and (4) covalent attachment of PEG macromolecules via an oxiran ring-opening process (Fig. 2).

Generation of free radicals on SR surfaces and functionalization with DS has been performed using a two-step procedure: generation of free radicals on SR surfaces and reaction of DS with the plasma-created sites. When inorganic or organic substrates are exposed to argon–plasma species, including electrons, ions, and neutrals, surface free radicals are generated. In a plasma environment, all surfaces are charged negative because the electrons have significantly higher mobility in comparison to their charged counterparts ($V_e/V_i = m_i/m_e$; where V_e and V_i are the electron and ion velocities and m_i and m_e stand for ion and electron masses, respectively) and reach faster on the surfaces that confine the discharge. However, charged surface species will instantly recombine (are neutralized) under open laboratory conditions (OLCs), and their lifetime is also very short in vacuum (*in situ*) environments. Plasma-produced free radical species will sur-

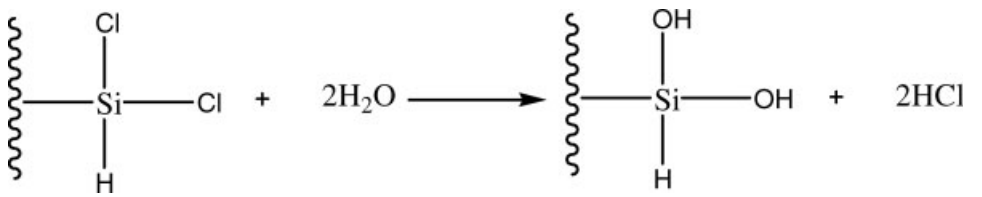

Scheme 3

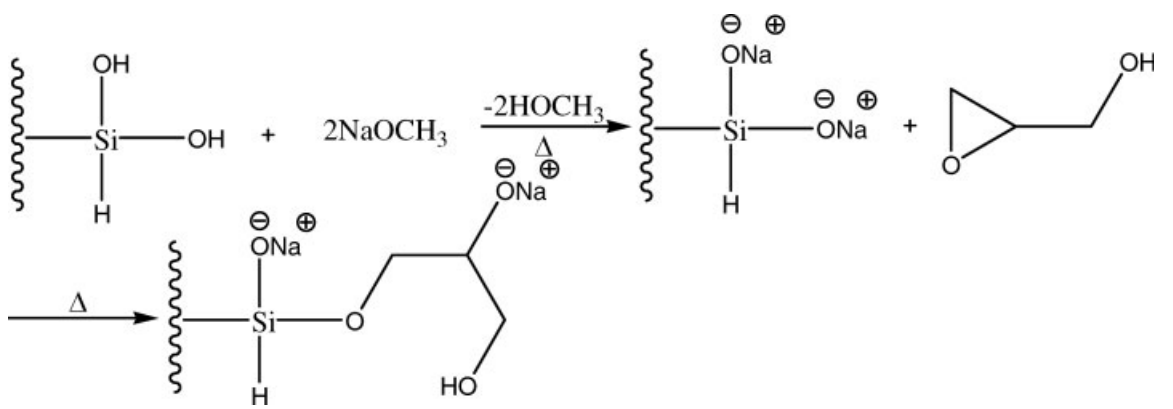

Scheme 4

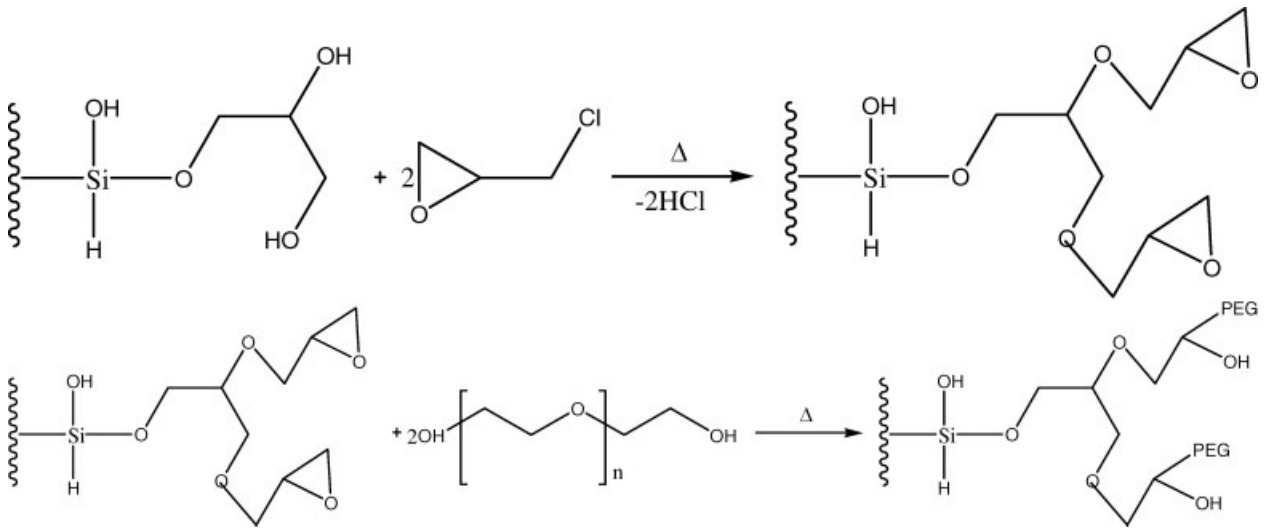

Scheme 5

vive longer under vacuum or inert gas environments in comparison to the charged entities.

Surface-attached free radical species can interact *in situ* (in the absence of plasma) even with non-functional (stable) molecules, including DS. This process will lead to the covalent implantation of SiH_xCl_y ($x < 2$ and $y < 2$) functionalities that are responsible for the generation of —Si—OH groups under OLCs. (Scheme 1).

This plasma-enhanced surface-functionalization approach of SR has not been reported yet to our knowledge.

Silicon–chlorine groups generated using plasma-enhanced functionalization readily react with —OH functionalities of PEG molecule in the absence of moisture. (Scheme 2).

Graft-polymerization of glycidol onto plasma-functionalized SR surfaces was performed in a two-step process. First, the DS-functionalized SR surfaces were washed with distilled water to generate —Si—OH end groups. (Scheme 3).

The sodium methoxide step is required to activate the OH groups and to promote the polymer brush formation process, and the samples were activated using sodium methoxide, and the procedure was repeated.[20] (Scheme 4).

It should be mentioned that a one-step polymerization process will result in the formation of linear PG structures, while repeating the earlier step, leading to branched, brush-type PG chains.

Oxirane-group terminated brushes were also prepared as structures required for anchoring PEG molecules. (Scheme 5).

Survey ESCA data resulting from TFAA-exposed SR and PEG 400- and PEG 600-coated SR substrates show a 0.4%, 5.1%, and 1.2% relative surface fluorine atomic concentration for untreated SR, PEG 400-, and PEG 600-coated SR samples, respectively (Fig. 3). The 0.4% relative fluorine atomic concentration of trifluoroacetic acid-treated SR is probably related to the presence of OH groups on the end of macromolecular chains. Different fluorine atomic concentration exhibited by the PEG 400- and PEG 600-coated substrates is attributed to the reduced diffusion of PEG 600 macromolecules into the functionalized surface layers, in comparison to PEG 400 during the grafting process, and as a result to the diminished covalent attachment of PEG-600 molecules to the activated substrate in comparison to PEG-400.

Figure 4 shows the HR C1s ESCA spectrum of SR [Fig. 4(A)], argon–plasma-treated SR [Fig. 4(B)], argon–plasma exposed and *in situ* DS-derivatized SR [Fig. 4(C)]. The presence of C—O (286.5 eV) BE peak in the diagram of both argon–plasma treated and

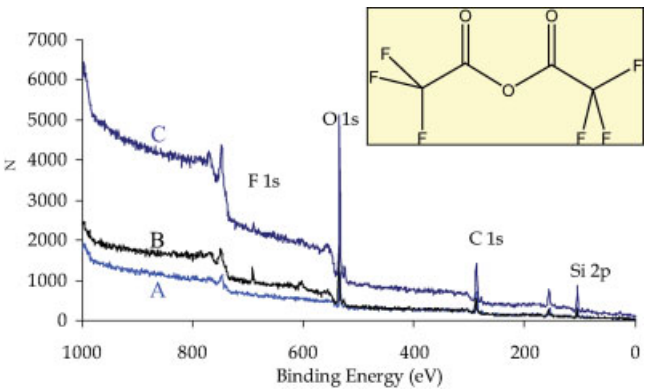

Figure 3 Survey ESCA spectra of TFAA-exposed untreated MSR (A), PEG 400-coated and TFAA-derivatized MSR (B), and PEG 600-coated and TFAA-derivatized MSR (C). [Color figure can be viewed in the online issue, which is available at www.interscience.wiley.com.]

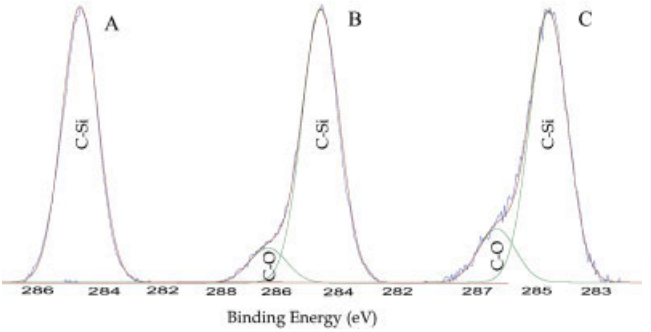

Figure 4 HR C1s ESCA spectra of MSR (A), Ar-plasma treated (B), and Ar-plasma treated and *in situ* DS-derivatized MSR (C).

DS-functionalized samples should be noted. Argon–plasma generated surface-free radicals readily to generate carbon- and oxygen-based functionalities, and surface-attached Si—Cl groups are converted into C—OH and Si—OH groups under OLCs.

Successful grafting of PEG molecules onto Si—Cl-functionalized surfaces can be concluded from C1s HR ESCA diagrams of modified SR substrates [Figs 5(A) and 5(B)]. The existence of a dominant surface area C—O BE peak in the ESCA diagram of PEG 400-grafted MSR is indicative of the development of an intensive grafting process. However, a significantly smaller surface area C—O BE peak can be identified in the ESCA diagram of PEG-grafted FSR. Grafting experiments, repeated several times for the attachment of PEG molecules onto DS-functionalized FSR surfaces, showed in all cases a lower grafting efficiency in comparison to the grafting efficiency of

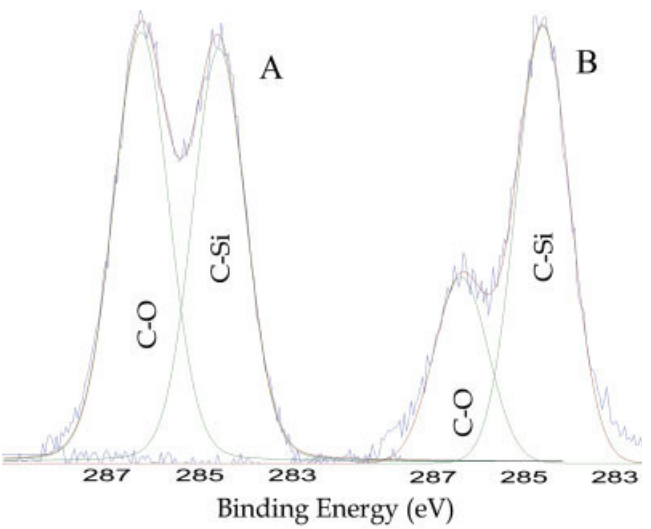

Figure 5 HR C1s ESCA spectra of PEG-grafted MSR (A) and PEG-grafted FSR (B).

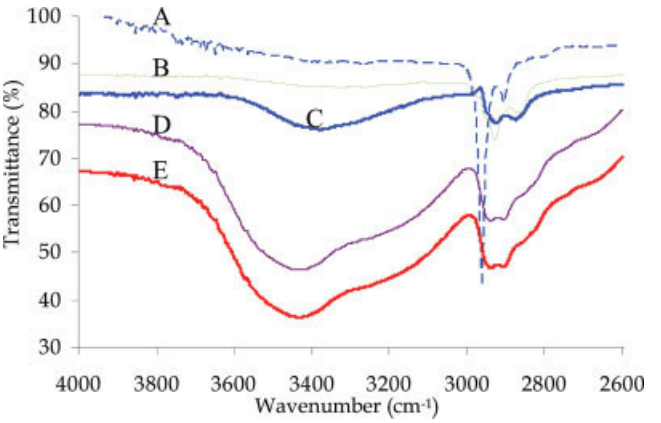

Figure 6 ATR-FTIR diagram of MSR (A), differential ATR-FTIR spectrum of PEG-grafted MSR (B), differential ATR-FTIR spectrum of linear PG -grafted MSR (C), polyvinyl alcohol (MW: 13,000–23,000) (D), and PEG (MW: 400) (E). [Color figure can be viewed in the online issue, which is available at www.interscience.wiley.com.]

the MSR substrate. It is suggested that lower molecular weight processing-origin additives, incorporated into the FSR that could be removed during the grafting procedure, might be responsible for this phenomenon.[22]

ATR-FTIR diagram of MSR, PEG and polyvinyl alcohol, and differential ATR-FTIR spectra of PEG- and PG-grafted MSR are presented in Figures 6–8. ATR-FTIR absorption assignments were performed according to IR data base.[23] The 2600–4000 cm^{-1} wavenumber region (Fig. 6) indicates the presence of characteristic asymmetrical and symmetrical stretching-mode absorptions of CH_3 groups (2962 and 2872 cm^{-1}) in the diagram of the unmodified MSR. The differential FTIR spectrum of PG-grafted MSR sub-

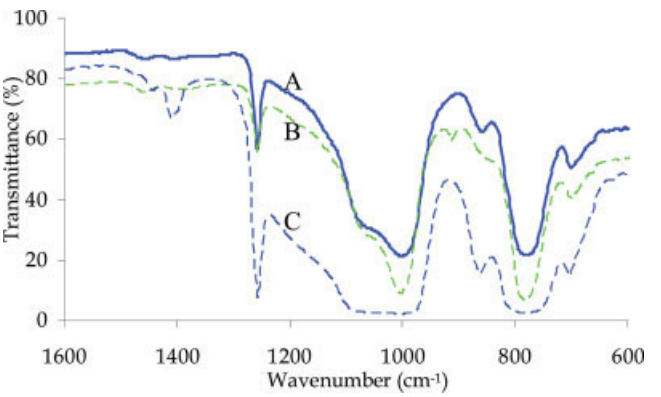

Figure 7 The ATR-FTIR diagram of differential ATR-FTIR spectrum of PG -grafted MSR (A), differential ATR-FTIR spectrum of PEG-grafted MSR (B) and MSR (C) in the 600–1600 cm^{-1} wavenumber range. [Color figure can be viewed in the online issue, which is available at www.interscience.wiley.com.]

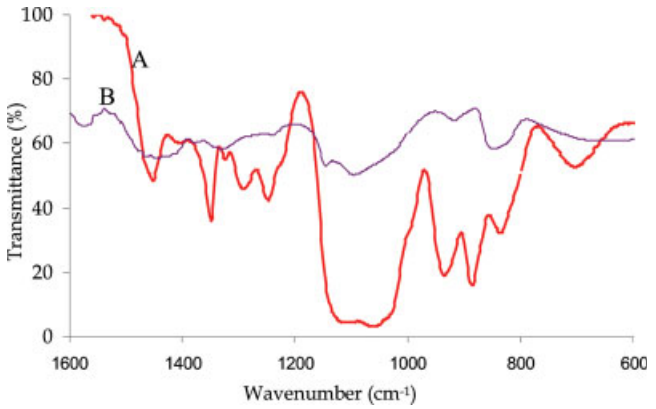

Figure 8 ATR-FTIR diagrams of PEG (MW: 400) (A) and polyvinyl alcohol (MW: 13,000–23,000) (B). [Color figure can be viewed in the online issue, which is available at www.interscience.wiley.com.]

strate reveals a broad and strong absorption in the 3200–3600 cm^{-1} wavenumber zone, which is indicative of the existence of intermolecularly hydrogen-bonded OH functionalities that is exhibited by the peculiar stretching frequencies. Owing to the thin film nature of PEG-grafted MSR, there is only a slight absorption in the 3200–3600 cm^{-1} wavenumber zone. This can be evidenced clearly by ATR-FTIR spectra, because poly(dimethylsiloxane) (PDMS) does not have a significant absorption in the 3200–3600 cm^{-1} wavenumber range. The relative surface area ratio of asymmetrical and symmetrical stretching absorption frequencies of the C—H groups is also different relative to the same surface area ratio of the unmodified MSR substrates. Peak surface areas of modified substrates are comparable, and shifted to significantly lower wavenumber values (2850 and 2926 cm^{-1}) corresponding to CH_2 and CH stretching vibrations, owing to the presence of PEG or PG layer on MSR surfaces.

The ATR-FTIR diagram of MSR, PEG-grafted MSR, and PG-grafted MSR in the 600–1600 cm^{-1} wavenumber range (Fig. 7) reveals less differences in the absorption patterns of MSR and PEG-coated samples. The presence of a strong and complex absorption region (700–900 cm^{-1}) characteristic of PDMS-based polymers is evident in the ATR-FTIR spectrum of MSR. The presence of a narrow 1258 cm^{-1} vibration assigned to the deformation vibration of methyl groups present in $>Si(CH_3)_2$ entities, and the existence of a strong and broad stretching vibration peak of the $—Si(CH_3)_2—$ groups, around 800 cm^{-1}, in addition to a very strong open chain, stretching —Si—O—Si— absorption (950–1100 cm^{-1}), because of the polymer backbone chain are characteristic for PDMS struc-

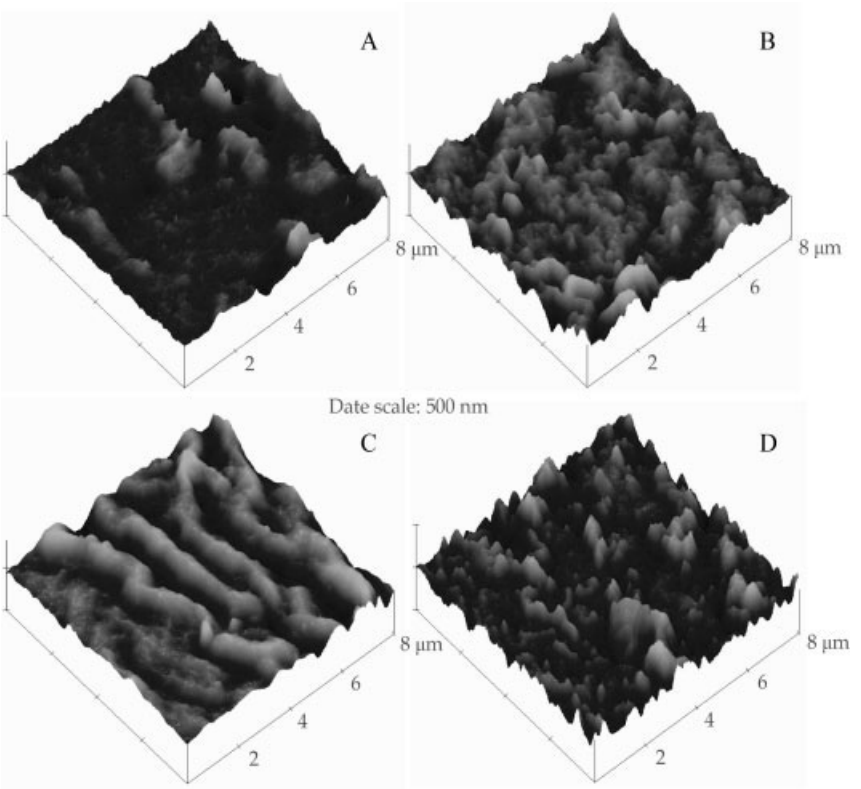

Figure 9 Contact-mode AFM images of untreated medical grade MSR (A), argon–plasma-treated and *in situ* DS-derivatized MSR (B), PEG-grafted (C) and PG-coated and subsequently PEG-grafted MSR (D).

tures. This can be related to the fact that the ATR-FTIR sampling depth is around 10–15 μm and to the thin layer nature of the modified MSR surface layers. Accordingly, the resulting spectrum is mainly composed of PDMS-origin vibrations. However, one can observe that the $>Si(CH_3)_2$ deformation vibration peak area is reduced, and the 800 and 1000 cm^{-1} peak areas are narrowed. These changes allow us to suggest that these vibrations appear as a result of a superimposition of ATR-FTIR diagrams of PDMS and PG structures. The presence of —C—O—C—, PDMS-origin —Si—O—Si— (950–1100 cm^{-1}), >C—OH (3100–3600 cm^{-1}), $—CH_2—CH—$ (2850–2930 cm^{-1}), and $—Si(CH_3)_2—$ (750–850 cm^{-1}) linkages in the PG structure make the ATR-FTIR diagrams of the coated MSR substrates apparently resemble the spectra of polyvinyl alcohol and PEG (Fig. 8).

It should be emphasized that due to the thin layer structure of the plasma-modified PDMS surface layers, the FTIR investigations should only be considered suggestive. Accordingly, FTIR analyses were not performed on oxirane-groups-terminated layers and on surface structures where PEG molecules were anchored as end chains using the oxirane functionalities.

Surface morphology changes as a result of the functionalization process are revealed by 3D and top-view AFM images (Figs. 9 and 10). Both contact- and tapping-mode operations were performed. During the contact-mode operation, the tip is in the vicinity of the sample surfaces where repulsive forces dominate (e.g., Coulomb potential) the tip–sample interaction. In the tapping or intermittent contact mode operation (where the tip touches the surface only for short periods of time), the repulsive forces control the tip–sample interaction; however, the amplitude of the oscillation of the tip is significantly higher (10–50 nm) in comparison to the noncontact mode (5 nm), where the attractive (e.g., van der Waals) forces control the tip–sample interaction. Accordingly, the tapping mode scanning will produce less damage to soft material surfaces, including polymers, biopolymers, etc.).

It can be observed that practically similar contact- and tapping-mode images were obtained. This indicates the presence of stable and fairly robust surface structures. It also should be mentioned that the small-grain structure surface topographies of MSR are replaced by large hill-valley-type structures because of the presence of covalently linked PEG 400 molecules on MSR surfaces.

The friction AFM images (Fig. 11) provide more information on the surface properties. Untreated, argon–plasma exposed and PEG-grafted images indicate the presence of weaker friction relative to the PG -coated substrates. Friction images reflect the interaction between the AFM cantilever-tip and the surface topography of the substrates.

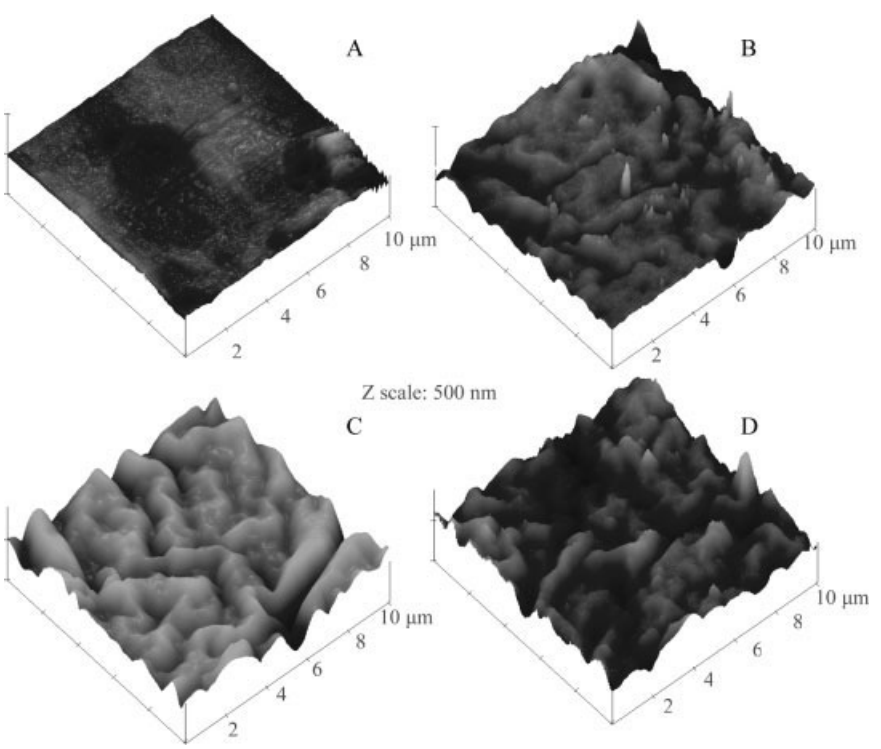

Figure 10 Tapping-mode AFM images of MSR (A) untreated, (B) argon–plasma followed by $SiCl_2H_2$ *in situ*, (C) PEG grafted, and (D) glycidol copolymerization.

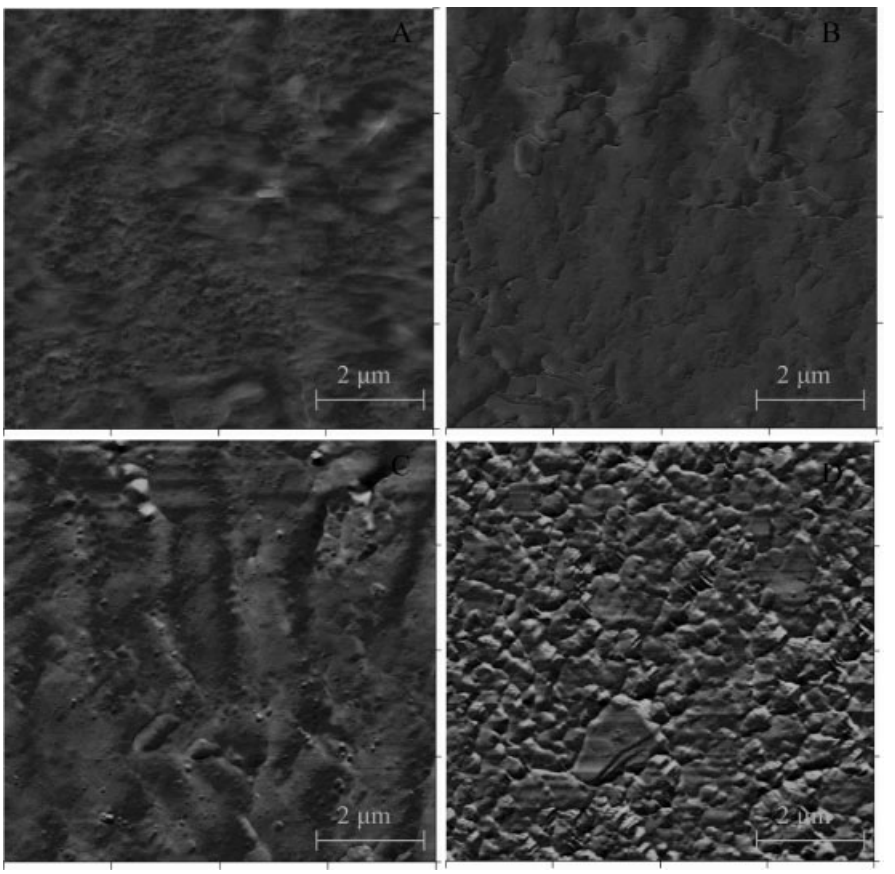

Figure 11 AFM friction spectra of MSR (A) untreated, (B) argon–plasma-treated followed by $SiCl_2H_2$ *in situ*, (C) PEG-grafted and (D) Glycidol copolymerization MSR.

The antifouling ability of PEG-coated MSR and FSR substrates are presented in Table I. The number of *L. monocytogenes* in the biofilm developed on PEG-coated MSR is nearly 1 log CFU/chip (90% reduction, $P < 0.05$) lower in comparison to the unmodified (control) substrates. However, there is much less decrease in the number of bacteria attached on the functionalized FSR. A less efficient attachment of PEG molecules onto the FSR surfaces is probably responsible for this behavior. It is noteworthy that even argon–plasma-treated and DS-functionalized SR substrates exhibit slight antifouling characteristics. Surface morphology changes generated as a result of the functionalization processes could have affected bacterial adhesion.

Survey ESCA diagram of linear PG-coated MSR substrates (Fig. 12) shows a 60.8% C, 28.2% O, and a 11.0% Si relative surface atomic concentration. This

TABLE I
Biofilm Formation by *L. monocytogenes* on Virgin and Modified MSR and FSR Substrates

	log CFU/chip	
Sample	Medical-grade silicone rubber (MSR)	Food-grade silicone rubber (FSR)
Virgin	3.96	4.08
Ar plasma-treated and *in situ* SiH_2Cl_2 derivatized	3.41	3.89
PEG-grafted	3.09	3.78

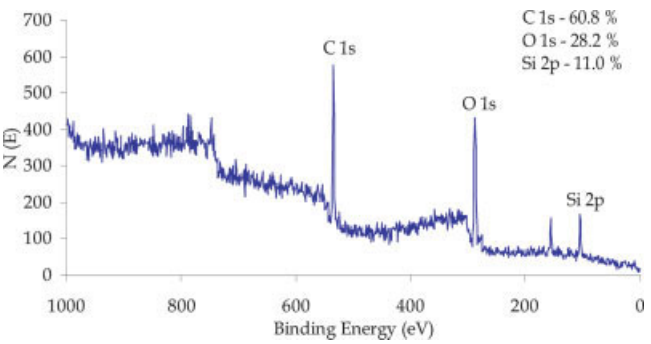

Figure 12 Survey ESCA spectrum of linear PG -grafted MSR. [Color figure can be viewed in the online issue, which is available at www.interscience.wiley.com.]

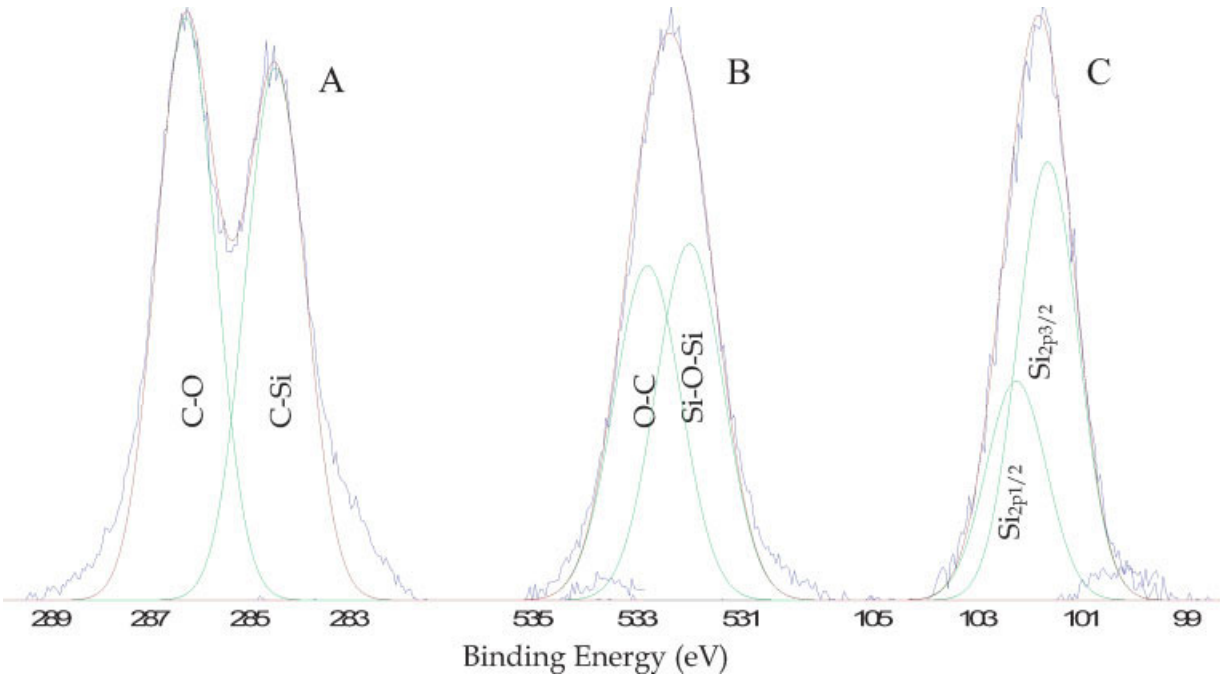

Figure 13 HR ESCA spectra of linear PG-grafted MSR: (A) C 1s, (B) O 1s, and (C) Si 2p. [Color figure can be viewed in the online issue, which is available at www.interscience.wiley.com.]

atomic composition compared to the atomic composition of MSR (50% C, 25% O, and 25% Si), is indicative that the MSR substrate surfaces were coated with a high C—and O—containing layer. The presence of a substrate-origin Si BE peak in the ESCA diagram shows that the deposited PG is a very thin layer. HR C1s diagrams [Fig. 13(A)] exhibit the presence of a dominant surface area C—O BE (286.5 eV) and C—C (285 eV) BE peaks, in addition to the Si—C peak (284.4 eV) that is still visible because of the thin layer nature of the deposited PG layer. Actually, the HR ESCA spectrum of polyvinyl alcohol (Fig. 14) is quite similar to that of the PG C1s diagram, except the C—Si (284.4 eV) BE peak is replaced for C—C (285 eV) BE. These findings substantiate the ATR-FTIR data that PG surface layers were deposited onto the argon–plasma-DS-functionalized SR substrate surfaces.

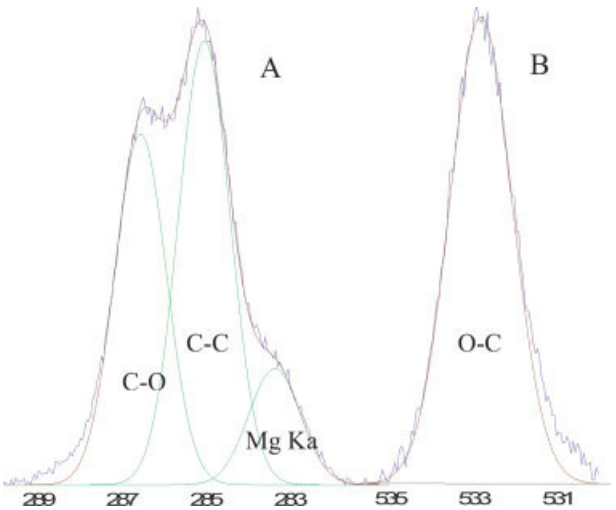

Figure 14 HR ESCA spectra of polyvinyl alcohol: (A) C 1s and (B) O 1s. [Color figure can be viewed in the online issue, which is available at www.interscience.wiley.com.]

The O1s HR ESCA diagrams [Fig. 13(B)] reveal a bimodal pattern. Deconvoluted peaks were assigned using the HR ESCA diagram of hydroxypropyl cellulose.[24] The presence in the O1s ESCA diagrams of the coated layers of a dominant C—OH/C—O—C (532.8 eV) peak and the existence of a 532 eV BE peak related to Si—O—Si linkages are obvious. Si 2p ESCA spectrum of PG-coated substrates [Fig. 13(C)] shows a symmetrical BE peak (101.6 eV), which is practically identical in BE shift to that of SR. This allows us to suggest that the SR backbone structure was not altered significantly during the surface modification process.

TABLE II
Biofilm Formation by *L. monocytogenes* on Virgin and Modified MSR Substrates

Sample	log CFU/chip
Virgin MSR	3.54
Ar plasma-treated and *in situ* SiH_2Cl_2 derivatized MSR	3.33
Linear polyglycidol-grafted MSR	3.47

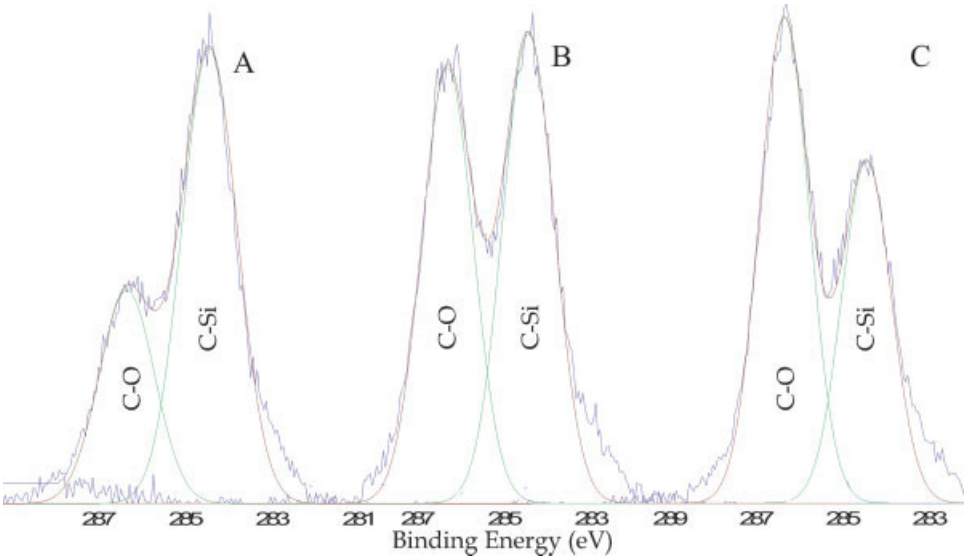

Figure 15 HR ESCA spectra of branched PG -grafted MSR: (A) C 1s, (B) O 1s, and (C) Si 2p. [Color figure can be viewed in the online issue, which is available at www.interscience.wiley.com.]

The antifouling ability of MSR substrates coated with linear PG and subsequently functionalized with PEG end chain molecules is shown in Table II. It is surprising that the number of *L. monocytogenes* on PG/PEG coated MSR is practically the same as compared to the control substrates.

Multistep grafting processes resulted in branched PG-structures which incorporate higher C—OH surface-densities. HR C1s ESCA diagrams of one-, two- and three-step-modified substrates show that higher the number of the functionalization steps larger the relative ratio of the C—O/C—C (Si—C) surface areas (Fig. 15).

The antifouling ability of branched PG-coated MSR substrates (three steps) are presented in Table III. The number of *L. monocytogenes* on PG-coated MSR is 0.5 log CFU/chip higher than that on the untreated substrates.

It is concluded that even if some of the —OH-groups bearing macromolecular structures, including polysaccharides, exhibit antifouling characteristics, the presence of —OH groups attached to the macromolecular chains is not sufficient for the generation of bacteria-repelling characteristics. Macromolecular conformation and conformational mobility associated with steric isomerism could also significantly influence the interaction between the OH-bearing structures and bacteria.

HR C1s ESCA data resulting from MSR coated with oxirane-groups-terminated PG brushes (Fig. 16) show

TABLE III
Biofilm Formation by *L. monocytogenes* on Branched Polyglycidol-Grafted MSR Substrates

Sample	log CFU/chip
Virgin MSR	3.84
Ar plasma-treated and *in situ* SiH_2Cl_2 derivatized MSR	3.49
Polyglycidol-grafted MSR synthesized in a three-step process	4.39

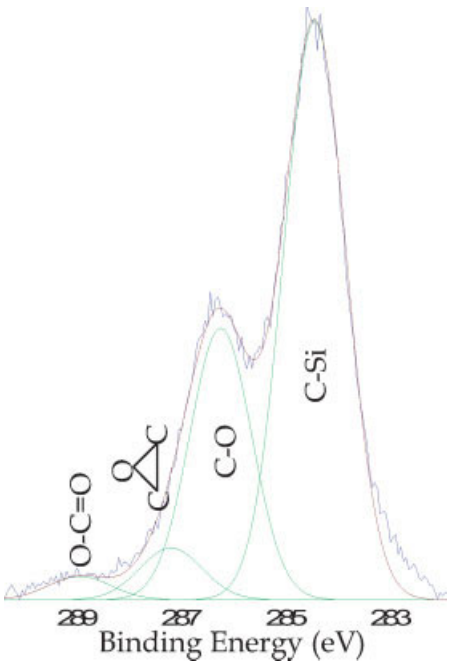

Figure 16 HR C1s XPS spectrum of ECH-functionalized and PG-grafted MSR. [Color figure can be viewed in the online issue, which is available at www.interscience.wiley.com.]

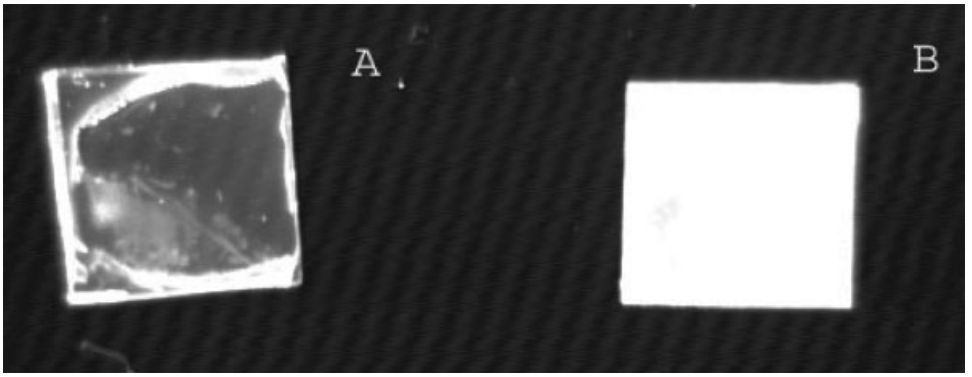

Figure 17 Fluorescence images of fluorescamine-derivatized (A) MSR and (B) modified (aminated) MSR.

the presence of a 287 eV (carbon atom incorporated in the oxirane ring) BE peak in addition to the characteristic C—O (286.5 eV) and C—C (285 eV) peaks. The ESCA spectrum of poly(glycidyl methacrylate)[24] was used to assign the oxirane-ring-related BE peaks. It was concluded that the covalent attachment of ECH, with reformation of the oxirane ring has been successfully accomplished. However, to obtain additional proof for the presence of oxirane end groups on the functionalized, washed, and vacuum-dried MSR surfaces (1 step/1-h reaction), *ex situ* amination using ethylene diamine, and subsequent fluorescamine-derivatization reaction were performed, both on the unmodified and modified substrates. Optical images (Fig. 17) clearly indicate the presence of a strong fluorescence only in the case of ECH-functionalized and subsequently aminated, modified MSR surfaces. The resulting fluorescamine complex substantiates the earlier conclusion that oxirane rings are covalently attached to the PG chains.

The antifouling ability of oxirane-terminated PG brush-coated MSR substrates is shown in Table IV. The number of *L. monocytogenes* on treated MSR is comparable to that of untreated substrates.

HR C_{1s} XPS results (Fig. 18) show the presence of a large surface area C—O (286.5 eV) BE peak that accompanies the ER-origin C—Si (284.4 eV) peak. ED-based fluorescamine test (absence of fluorescence) also indicates that the oxirane rings were involved into the PEG attachment reactions. These results suggest a potentially novel approach for the development of a multistep grafting process through a ring-opening reaction mechanism.

Surprisingly, biofilm formation on PEG-grafted MSR surfaces was not reduced (Table IV). It is concluded that even the presence of PEG chains on linear PG intermediate layer does not guarantee an antifouling ability.

TABLE IV
Biofilm Formation by *L. monocytogenes* on PG-Coated and PEG-Grafted MSR Substrates

Sample	log CFU/chip
Virgin MSR	3.80
Polyglycidol-grafted MSR	3.82
Oxirane-terminated MSR	3.68
Oxirane-terminated and PEG-grafted MSR	3.91

CONCLUSIONS

It was shown that the attachment of PEG molecules onto the Si—Cl-bearing substrate surfaces is more efficient in the case of MSR in comparison to FSR. The presence of processing additives in the FSR samples is

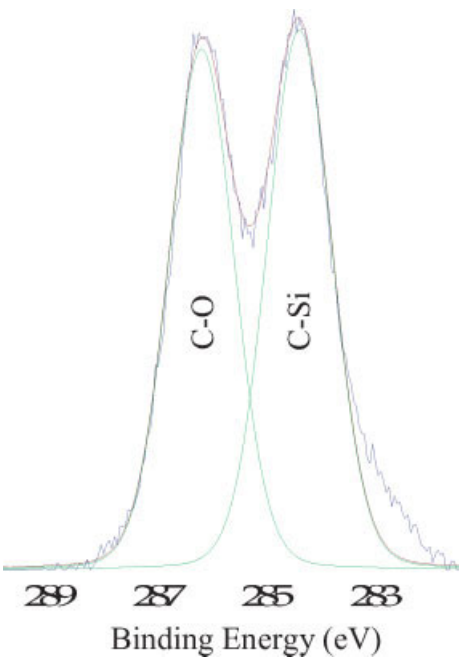

Figure 18 HR C1s XPS spectrum of oxirane-terminated and PEG-grafted MSR. [Color figure can be viewed in the online issue, which is available at www.interscience.wiley.com.]

suggested to be responsible for the development of a less efficient grafting process. This was also reflected in the antifouling behavior of the two functionalized MSR and FSR substrates. A significantly more pronounced antifouling behavior is associated with the PEG-bearing MSR samples relative to FSR substrates.

MSR substrates coated with covalently attached PG layers did not exhibit antifouling characteristics, and even retained higher bacteria number than do unmodified MSR samples. This allows us to suggest that even if some —OH decorated macromolecular structures, such as polysaccharides, exhibit antifouling behavior, the presence of a significant number of —OH functionalities is not enough to generate bacteria-repelling properties. Tangled macromolecular chains having —OH groups, and incorporated into surface-layer structures, might favor entrapment of bacterial cells. Macromolecular conformation and conformational mobility, and the availability of OH groups, could play an important role in the interaction of biomolecules and bacterial cells with the newly generated surface layers.

It was demonstrated that even if the PG structures are ''decorated'' with PEG, the antifouling activity of the resulting structures is not improved. These findings indicate that only PEG directly connected to the SR-functionalized surfaces exhibit antifouling behavior.

References

1. Daveyand, M. E.; O'Toole, G. A. Microbiol Mol Biol Rev 2000, 64, 847.
2. Carpentierand, B.; Cerf, O. J Appl Bacteriol 1993, 75, 499.
3. Bos, R.; van der Meiand, H. C.; Busscher, H. J. FEMS Microbiol Rev 1999, 23, 179.
4. Stanley, P. M. Can J Microbiol 1983, 29, 1493.
5. Marshall, K. C.; Stoutand, R.; Mitchell, R. J Gen Microbiol 1971, 68, 337.
6. Park, K. D.; Kim, Y. S.; Han, D. K.; Kim, Y. H.; Lee, E. H. B.; Suhand, H.; Choi, K. S. Biomaterials 1998, 19, 851.
7. Harris, J. M. Poly(ethylene glycol) Chemistry: Biotechnical and Biomedical Application; Harris, J. M., Ed.; Plenum: New York, 1992, Chap. 1, p. 1.
8. Osterberg, E.; Bergstrom, K.; Holmberg, K.; Schuman, T. P.; Riggs, J. A.; Burns, N. L.; Vanalstineand, J. M.; Harris, J. M. J Biomed Mater Res 1995, 29, 741.
9. Ista, L. K.; Fan, H. Y.; Bacaand, O.; Lopez, G. P. FEMS Microbiol Lett 1996, 142, 59.
10. Field, J. B.; Toprakcioglu, C.; Ball, R. C.; Stanley, H. B.; Dai, L.; Barford, W.; Penfold, J.; Smithand, G.; Hamilton, W. Macromolecules 1992, 25, 434.
11. Taunton, H. J.; Toprakcioglu, C.; Fettersand, L. J.; Klein, J. Macromolecules 1990, 23, 571.
12. Akizaw, M. A.; Kino, T. K.; Koshikawa, S.; Ikada, Y.; Kishida, A.; Yamashitaand, M.; Imamura, K. Trans Am Soc Artif Intern Organs 1989, 35, 333.
13. Zalipskyand, S.; Harris, J. M. Poly(ethylene glycol): Chemistry and Biological Applications (ACS Symposium series), Harris, J. M.; Zalipsky, S., Ed.; American Chemical Society: Washington, DC, 1997; Chap. 1, p 1.
14. Amijiand, M.; Park, K. J Biomater Sci Polym Ed 1993, 4, 217.
15. Cosnier, S. Biosens Bioelectron 1999, 14, 443.
16. Gombotz, W. R.; Wang, G.; Horbettand, T. A.; Hoffman, A. S. Poly(ethylene glycol) Chemistry: Biotechnical and Biomedical Applications, Harris, J. M., Ed.; Plenum: New York, 1992, Chap. 16, p 247.
17. Gombotz, W. R.; Guanghui, W.; Horbettand, T. A.; Hoffman, A. S. In Poly(ethylene glycol) Chemistry: Biotechnical and Biomedical Applications, Plenum: New York, 1992.
18. Han, D. K.; Parkand, K. D.; Kim, Y. H. J Biomater Sci Polym Ed 1998, 9, 163.
19. Kiff, F. T.; Richardsand, R. W.; Thompson, R. L. Langmuir 2004, 20, 4465.
20. Khanand, M.; Huck, W. T. S. Macromolecules 2003, 36, 5088.
21. Denes, A. R.; Somers, E. B.; Wongand, A. C. L.; Denes, F. J Appl Polym Sci 2001, 81, 3425.
22. Langowskiand, B. A.; Uhrich, K. E. Langmuir 2005, 21, 6366.
23. Bellamy, L. J. The Infrared Spectra of Complex Molecules; Wiley: New York, 1966.
24. Bemsonand, G.; Briggs, D. High Resolution XPS of Organic Polymers: The Scienta ESCA300 Database; Wiley: Chichester, 1992.